Bai Liangyu[1], Tang Houjun, Liu Chao

Key Laboratory of Control of Power Transmission and Transformation, Ministry of Education，Shanghai Jiao Tong University

Bi-directional Contactless Inductive Power Transfer System Modeling and verifying

Abstract. *This paper presents an approach for the modeling of bi-directional contactless inductive power transfer (CIPT) system based on the generalized state space averaging (GSSA) method. By using the proposed method, a dynamic model can be realized by a linear model. The validity of the model is verified by theoretical analysis, simulations and experimental results of a 2kW prototype bi-directional CIPT system with a 1mm air-gap. Results indicate that the proposed model is an ideal analysis tool for CIPT system .*

Streszczenie. *Zaprezentowano system bezprzewodowej, dwukierunkowej transmisji mocy CIPT. Metoda była zweryfikowana teoretycznie, przez symulacje oraz eksperymentalnie w systemie transmisji mocy 2 kW przez szczelinę 1 mm. (**Dwukierunkowa bezprzewodowa transmisja mocy – model i eksperymentalna weryfikacja**)*

Keywords: Bi-directional Contactless Inductive Power Transfer, Generalized State Space Averaging Method, dynamic model, steady state model.
Słowa kluczowe: beprzewodowa transmisja mocy

Introduction

Energy crisis is threatening people with the depletion of fossil energy, save energy and reduce the cost, increase resource utilization rate and reduce waste are major worldwide concerns [1]-[3]. Therefore, techniques for charging and discharging of electric equipments with the emphasis on simplicity, low cost, convenience, high efficiency and flexibility, have become the main focus of current research in both industrial and academic community.

The magnetic field has widely used for the transfer of power or information. Inductive contactless power transfer (CIPT) systems are designed to deliver power efficiently from a primary source to a secondary load over relatively large air gaps via magnetic coupling. According to CIPT system literature, with various circuit topologies and control method have been proposed, which range from very low power bio-medical implants to high power electric vehicle systems [4]-[10]. Most of these papers have specifically been designed for uni-directional power flow [4]-[12], and are not suitable for regenerative equipment, which require bi-directional power flow. A bi-directional inductive power transfer system has symmetric structure, can be realized by using two identical uni-directional inductive power transfer system. Bi-directional CIPT techniques are emerging as a viable choice as they meet most of the above attributes [13].

Traditionally, the performance of CIPT system is based on the T equivalent model [14] [15] and the mutual inductance coupling model[16]. The generalized state space averaging (GSSA) method proposed by Sanders is valid for modeling a wider range of converters [11], and the GSSA model of uni-directional CIPT developed by Fang Wan appears the most successful[17][18]. In essence, CIPT systems are typically nonlinear resonant power electronic converter systems, the GSSA method is valid for both steady state and dynamic analysis, and the order of a GSSA model can be determined according to the variable characteristics and required accuracy. However, to date no work has been reported to model bi-directional CIPT system which valid for both steady state and dynamic analysis.

Bi-directional CIPT is an ideal power interface for contactless integration of electric vehicles into typical power networks. The electrical model of system has been introduced in Section Ⅱ. And the generalized state space averaging method is analyzed in Section Ⅲ. Simulation results and experimental results of the CIPT is given in Section Ⅳ. Finally, conclusions are summarized in Section Ⅴ.

Electrical Model of CIPT System

A bi-directional CIPT system, with double directional power flow, is shown in Fig.1 (a). The primary and secondary circuits are implemented with virtually symmetrical topology, which include a reversible rectifier and a compensation circuit, to facilitate bi-directional power flow between the primary and secondary circuit. Each reversible rectifier is operated either in the inverting or rectifying mode, depending on the direction of the power flow. Where M represents the magnetic coupling or mutual inductance between L_1 and L_2 .A simplified circuit, omitting the grid side converter and representing the electrical equipment as DC sources, is shown in Fig.1 (b).

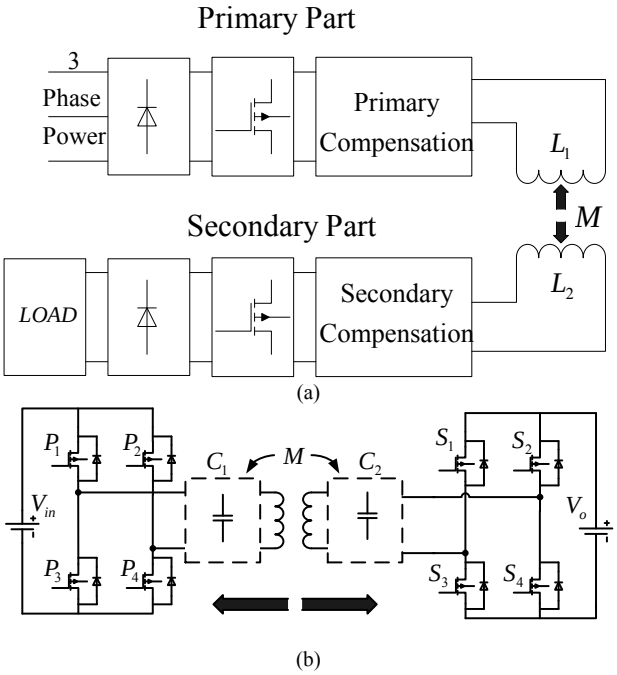

Fig. 1. (a) Bi-directional CIPT schematic; (b)Simplified circuit of the bi-directional CIPT schematic.

In uni-directional CIPT, four basic compensation topologies labeled as SS, SP, PP, and PS, where the first S or P stands for series or parallel compensation of the primary winding and the second S or P stands for series or parallel compensation of the secondary winding [11]. Considering the bi-directional CIPT has virtually symmetrical topology, the SS and PP topologies are chosen. The bi-directional CIPT system delivery mode at

steady state can be represented by the model in Fig.2 which the power flow direction is primary part to secondary part. The feed mode similar which power flow direction is reversed.

In addition, two assumptions are needed for the equivalent circuit: the switching devices are ideal and the load current is continuous in the secondary winding.

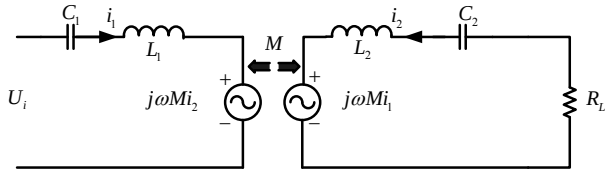

Fig. 2. Equivalent coupling circuit, with SS compensation topology.

From Fig.2, the actual state space variables are the Fourier coefficients of the circuit state variables, which are i_1, v_{C1}, i_2 and v_{C2}, according to Kirchoff's circuit laws, the equivalent circuit equations are then as follows (see List of Symbols for a description of all variables)

$$(1)\qquad \begin{cases} U_i = L_1\dfrac{di_1}{dt} + v_{C1} + j\omega M i_2 \\ i_1 = C_1\dfrac{dv_{C1}}{dt} \\ j\omega M i_1 = -L_2\dfrac{di_2}{dt} + v_{C2} + R_L i_2 \\ -i_2 = C_2\dfrac{dv_{C2}}{dt} \end{cases}$$

where $U_i = \mathrm{sgn}(t)U_{in}$, sgn(t) can be expressed as:

$$(2)\qquad \mathrm{sgn}(t) = \begin{cases} 1 & m\mathrm{T} \le t \le (2m+1)T/2 \\ -1 & (2m+1)\mathrm{T}/2 \le t \le (m+1)T \end{cases}$$

GSSA Model

In this section, some of the results of GSSA and their implications will be reviewed [16]-[18]. The GSSA method is based on a sliding window representation of dynamic variables, any waveform $x(t)$ can be approximated on a time interval $(t-T,t]$ to arbitrary accuracy with a Fourier series representation of the form:

$$(3)\qquad x(t) = \sum_{k=-\infty}^{\infty} \langle x\rangle_k(t) e^{jkwt}$$

Where the sum is over all integers $k, \omega = 2\pi/T$, and $\langle x\rangle_k(t)$ are the complex Fourier coefficients which are functions of time and are given by:

$$(4)\qquad \langle x\rangle_k(t) = \frac{1}{T}\int_0^T x(t-T+\tau)e^{-jkw(t-T+\tau)}d\tau$$

The terms $\langle x\rangle_k(t)$ determine the time-evolution of these Fourier coefficients as a window of length T slides over the actual waveform. Our approach to evaluate these is to determine an appropriate state-space model in which the coefficients as state variables. Certain properties of the Fourier coefficients are detailed below:

$$(5)\qquad \frac{d}{dt}\langle x\rangle_k(t) = \left\langle \frac{d}{dt}x \right\rangle_k(t) - jk\omega\langle x\rangle_k(t)$$

$$(6)\qquad \langle xy\rangle = \sum_i \langle x\rangle_{k-i}\langle y\rangle_i$$

Using first order approximation to obtain i_1, v_{C1}, i_2 and v_{C2}, the state variables can be shown as:

$$(7)\qquad \begin{cases} \langle i_1\rangle_1 = x_1 + jx_2 \\ \langle v_{C1}\rangle_1 = x_3 + jx_4 \\ \langle i_2\rangle_1 = x_5 + jx_6 \\ \langle v_{C2}\rangle_1 = x_7 + jx_8 \end{cases}$$

The zero-order coefficient are:

$$(8)\qquad \langle i_1\rangle_0 = x_9, \langle v_{C1}\rangle_0 = x_{10}, \langle i_2\rangle_0 = x_{11}, \langle v_{C2}\rangle_0 = x_{12}$$

The first-order coefficients have the following propriety:

$$(9)\qquad \begin{cases} \langle i_1\rangle_1 = \langle i_1\rangle_{-1}^* \\ \langle v_{C1}\rangle_1 = \langle v_{C1}\rangle_{-1}^* \\ \langle i_2\rangle_1 = \langle i_2\rangle_{-1}^* \\ \langle v_{C2}\rangle_1 = \langle v_{C2}\rangle_{-1}^* \end{cases}$$

It is straightforward to construct equivalent circuit realizations of the 4 coupled differential equations that represent the dynamics of the index-0 and index-1 Fourier coefficients of the CIPT. The coupled differential equations in state-space form have the following structure:

$$(10)\qquad \frac{d}{dt}\begin{bmatrix}\langle x\rangle_0 \\ \langle x\rangle_1\end{bmatrix} = \underbrace{\begin{bmatrix}A_1 & A_2 \\ A_3 & A_4\end{bmatrix}}_{A}\begin{bmatrix}\langle x\rangle_0 \\ \langle x\rangle_1\end{bmatrix} + \begin{bmatrix}0 \\ b\end{bmatrix}U_{dc}$$

The matrices A_1, A_2, A_3, A_4 and b are found to be:

$$(11)\qquad A_1 = \begin{bmatrix} 0 & -\dfrac{1}{L_1} & \dfrac{-j\omega M}{L_1} & 0 \\ \dfrac{1}{C_1} & 0 & 0 & 0 \\ \dfrac{-j\omega M}{L_2} & 0 & \dfrac{R_2}{L_2} & -\dfrac{1}{L_2} \\ 0 & 0 & \dfrac{1}{C_2} & 0 \end{bmatrix}$$

$$(12)\qquad A_2 = A_3 = 0$$

$$(13)\qquad A_4 = \begin{bmatrix} 0 & \omega & -1/L_1 & 0 \\ -\omega & 0 & 0 & -1/L_1 \\ 1/C_1 & 0 & 0 & \omega \\ 0 & 1/C_1 & -\omega & 0 \\ 0 & \omega M/L_1 & 0 & 0 \\ -\omega M/L_1 & 0 & 0 & 0 \\ 0 & 0 & 0 & 0 \\ 0 & 0 & 0 & 0 \end{bmatrix}$$

$$\begin{bmatrix} 0 & \omega M/L_1 & 0 & 0 \\ -\omega M/L_1 & 0 & 0 & 0 \\ 0 & 0 & 0 & 0 \\ 0 & 0 & 0 & 0 \\ -R_2/L_2 & \omega & -1/L_2 & 0 \\ -\omega & -R_2/L_2 & 0 & -1/L_2 \\ 1/C_2 & 0 & 0 & \omega \\ 0 & 1/C_2 & -\omega & 0 \end{bmatrix}$$

$$(14)\qquad b = \begin{bmatrix}0 & -2/\pi L_1 & 0 & 0 & 0 & 0 & 0 & 0\end{bmatrix}^T$$

where $\langle x\rangle_0$ and $\langle x\rangle_1$ representing the zero-order and first-order state variables, respectively, as column vectors defines by:

(15) $$\langle x \rangle_0 = [x_9 \quad x_{10} \quad x_{11} \quad x_{12}]^T$$

(16) $$\langle x \rangle_1 = [x_1 \quad x_2 \quad x_3 \quad x_4 \quad x_5 \quad x_6 \quad x_7 \quad x_8]^T$$

The zero-order average yields the state-space averaging model, in Equation (2), by applying the time derivative property of Fourier coefficients, it can be shown as:

(17) $$\langle \mathrm{sgn}(t) \rangle_0 = 0, \ \langle \mathrm{sgn}(t) \rangle_1 = -2j/\pi$$

Because submatrices A_2 and A_3 vanish, the fundamental component state-space averaging model and dynamic model decoupled from each other, zero-order steady state averaging model is shown as:

(18) $$\frac{d}{dt}\langle x \rangle_0 = A_1 \langle x \rangle_0$$

The first-order dynamic model of the system is:

(19) $$\frac{d}{dt}\langle x \rangle_1 = A_4 \langle x \rangle_1 + bU_{dc}$$

And can be expressed as below in:

(20) $$\begin{cases} i_1 = 2x_1 \cos \omega t - 2x_2 \sin \omega t \\ v_{C1} = 2x_3 \cos \omega t - 2x_4 \sin \omega t \\ i_2 = 2x_5 \cos \omega t - 2x_6 \sin \omega t \\ v_{C2} = 2x_7 \cos \omega t - 2x_8 \sin \omega t \end{cases}$$

It turns out that there is a difference between the zero-order and first-order dynamics, which suggests some potential decouplings and simplifications of the full model. These issues are discussed in next section.

Simulation and Experimental Results of the System

In this paper, the parameters used were $f = 40kHz$, $L_1 = 130\mu H$, $L_2 = 130\mu H$, $C_1 = 0.2\mu F$, $C_2 = 0.2\mu F$, $R_L = 27\Omega$, $V_{in} = 100V$.

Figure 3 shows the results of using the exact time domain and the GSSA model to simulate the delivery mode CIPT system, the feed mode CIPT similar. The GSSA model can accurately show the running characteristics of CIPT system, therefore, using this method is a superior tool for system design than those previously available.

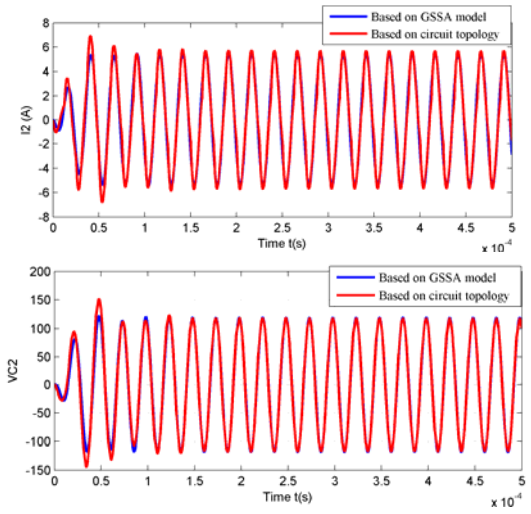

Fig. 3. Simulation results between circuit state variables i_2, v_{C2} of CIPT system by circuit topology and GSSA method.

The curves shown by blue lines are based on the GSSA model, and red lines are based on the circuit topology which is using the Simulink toolbox. Comparing the curves in Fig.3, all the state curves based on the GSSA method are very similar to those based on the exact time domain model, shows very good agreement.

In order to verify the viability of the proposed bi-directional CIPT system, a prototype 2kW CIPT system shown in Fig.4, was built and its performance was compared with simulations using GSSA model and circuit topology. The design parameters of the prototype, which has an efficiency of 90% with 1mm air gap.

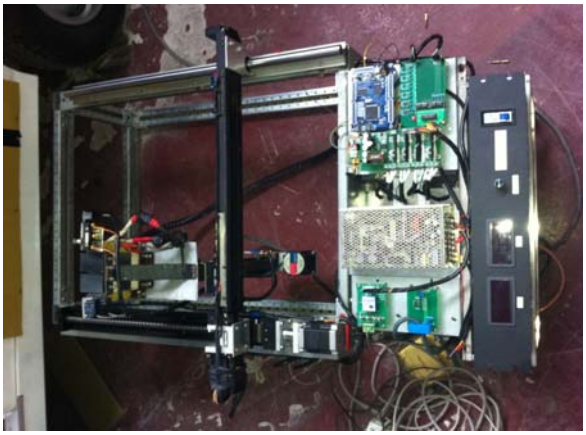

Fig.4. The 2kW CIPT system

Fig.5 shows the measured waveforms in a situation which is similar to simulated electric parameters in Fig.4. As can be seen from Fig.3 and Fig.5, the good agreement between simulated and measured results confirms the validity of the GSSA model analysis.

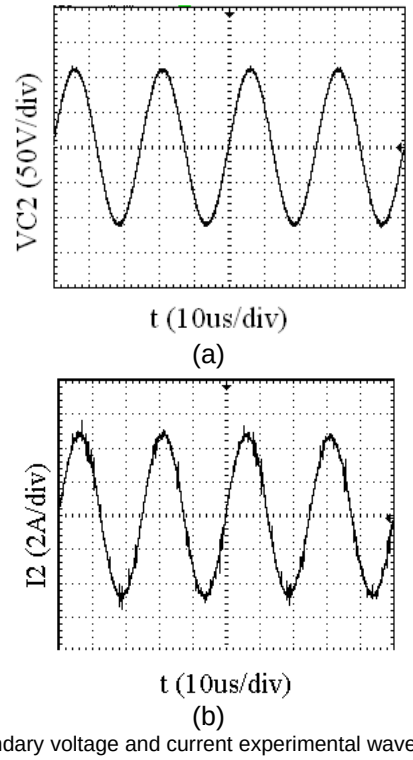

Fig.5 Secondary voltage and current experimental waveforms

Conclusion

In this paper, GSSA (Generalized State Space Averaging) method has been successfully used in modeling bi-directional CIPT system. The results obtained from the GSSA models are in good agreement with exact time domain simulation and experimental result based on the circuit topology. The analysis based on the GSSA model is more convenient and faster compared to circuit topology simulation or any other numerical simulation technique.

REFERENCES

[1]. M. H. Nehrir, C. Wang, and S. R. Guda, Alternative Energy Distributed Generation: Need for Multi-Source Operation, Proc. of North American Power Symposium, 2006, pp. 547-551.

[2]. R. Ramakumar and P. Chiradeja, Distributed generation and renewable energy ststems, Proc. of IEEE Energy Conversion Engineering Conf., 2002, pp. 716-724.

[3]. J. Balakrishnan, Renewable Energy and Distributed Generation in Rural Villages, Proc. of IEEE Industrial and Information Systems Conf., 2006, pp. 190-195.

[4]. Schuder, J. C., Powering an artificial heart: birth of the inductively coupled-radio frequency system in 1960, Artif. Organs. vol. 26 n. 11, pp. 909-915, November 2002.

[5]. Kelley, A. W., Owens, W. R., Connectorless power supply for an aircraft-passenger entertainment system, IEEE Trans. Power Electron., vol. 4 n. 3, pp. 348-354, 1989.

[6]. Egan, M. G., O' Sullivan, D. L., Hayes, J. G., Willers, M. J., Henze, C. P., Power-factor-corrected single-stage inductive charger for electric vehicle batteries, IEEE Trans. Ind. Electron., vol. 54 n. 2, pp. 1217-1226 2007.

[7]. Hirai, J., Kim, T.W., Kawamura, A. Wireless transmission of power and information for cableless linear motor drive, IEEE Trans. on Power Electron., vol. 15 n. 1, pp. 21-26 2000.

[8]. Kawamura, A., Ishioka, K., Hirai, J., Wireless transmission of power and information through one high-frequency resonant AC link inverter for robot manipulator application, IEEE Trans. On Ind. Appl., vol. 32 n. 3, Appl. 1996, pp. 503-508.

[9]. Jackson, D.K. Inductively-coupled power transfer for eletromechanical systems, Ph.D dissertation, Massachusetts Institute of Technology, U.S.A. 1998.

[10]. Albert, E., Contactless charging and communication for electric vehicles, IEEE Industry Applications Magazine, vol. 1 n.6, 1995, pp: 4-11.

[11]. Chwei-Sen Wang, Covic, G. A., Stielau, O. H. Power transfer capability and bifurcation phenomena of loosely coupled inductive power transfer systems, IEEE Trans. Ind. Electron., vol. 51 n. 1, pp. 148-156, February 2004.

[12]. Chwei-Sen Wang, Stielau, O. H. and Covic, G. A. Design considerations for a contactless electric vehicle battery charger, IEEE Trans. Ind. Electron., vol. 52 n. 5, pp. 1308-1314, October 2005.

[13]. U.K. Madawala and D. J. Thrimawithana, A two-way inductive power interface for single loads, Proc. of IEEE Industrial Technology Conf., 2010, pp.673-678.

[14]. H. H. Wu, A. P. Hu, S. C. Malpas, and D. M. Budgett, Determing optimal tuning capacitor values of TET system for achieving maximum power transfer, Electronics Letters, vol. 45, pp. 448-449, Apr 2009.

[15]. J. Gyu Bum and B. H. Cho, An energy transmission system for an artificial heart using leakage inductance compensation of transcutaneous transformer, Power Electronics, IEEE Transactions on, vol. 13, pp. 1013-1022, 1998.

[16]. Sanders, S. R., Noworolski, J. M., Liu, X. Z. and Verghese, G. C., Generalised averaging method for power conversion circuits, IEEE Transactions on Power Electronics, vol. 6 n. 2, April, 1991.

[17]. Wan Fang, Wei Liu, Jie Qian, Houjun Tang and Pengsheng Ye, Modeling and simulation of a transcutaneous energy transmission system used in artificial organ implants, Artif. Organs. vol. 33 n. 12, pp. 1069-1074, 2009.

[18]. Wan Fang, Houjun Tang, and Wei Liu, Modeling and analyzing an inductive contactless power transfer system for artificial hearts using the generalized state space averaging method, Journal of Computational and Theoretical Nanoscience, vol. 4, pp. 1-5, 2007.

Bai Liangyu was born in Shanxi province, China, in 1983. He received the B.S. degree in electrical engineering from Yanshan University, Qinhuangdao, China, in 2004, and M.S. degree in electrical engineering from Guangxi University, Nanning, in 2008. He is currently working toward his Ph.D. degree in electrical engineering at Shanghai Jiao Tong University.

His research interests include power electronics and wireless power transfer.

Tang Houjun was born in Shandong province, China, in 1957. He received B.S. and M.S. degrees in 1982 and 1988 respectively. He received Ph.D. degree in Yamagata University, Japan, 1997. He is Professor of the Department of Electrical Engineering, Shanghai Jiao Tong University.

His current research interests include automotive electronics, wireless power transfer.

Liu Chao was born in Shandong province, China, in 1988. He is currently working toward his Master degree in electrical engineering at Shanghai Jiao Tong University.

His research interests include power electronics and wireless power transfer.